

Lattice Boltzmann based discrete simulation for gas-solid fluidization

Limin Wang^{a,*}, Bo Zhang^{a,b}, Xiaowei Wang^a, Wei Ge^a, Jinghai Li^a

^aThe EMMS Group, State Key Laboratory of Multiphase Complex Systems, Institute of Process Engineering, Chinese Academy of Sciences, Beijing 100190, China

^bState Key Laboratory of Organic-Inorganic Composites, Beijing University of Chemical Technology, Beijing 100029, China

Abstract

Discrete particle simulation, a combined approach of computational fluid dynamics and discrete methods such as DEM (Discrete Element Method), DSMC (Direct Simulation Monte Carlo), SPH (Smoothed Particle Hydrodynamics), PIC (Particle-In-Cell), etc., is becoming a practical tool for exploring lab-scale gas-solid systems owing to the fast development of parallel computation. However, gas-solid coupling and the corresponding fluid flow solver remain immature. In this work, we propose a modified lattice Boltzmann approach to consider the effect of both the local solid volume fraction and the local relative velocity between particles and fluid, which is different from the traditional volume-averaged Navier-Stokes equations. A time-driven hard sphere algorithm is combined to simulate the motion of individual particles, in which particles interact with each other via hard-sphere collisions, the collision detection and motion of particles are performed at constant time intervals. The EMMS (energy minimization multi-scale) drag is coupled with the lattice Boltzmann based discrete particle simulation to improve the accuracy. Two typical fluidization processes, namely, a single bubble injection at incipient fluidization and particle clustering in a fast fluidized bed riser, are simulated with this approach, with the results showing a good agreement with published correlations and experimental data. The capability of the approach to capture more detailed and intrinsic characteristics of particle-fluid systems is demonstrated. The method can also be used straightforward with other solid phase solvers.

Keywords: Discrete particle simulation, Lattice Boltzmann method, Computational fluid dynamics, Fluidization, Multiphase flow, Simulation

1. Introduction

Gas-solid fluidization systems are widely encountered in both physical and chemical processes for many industries, for instance, fluid catalytic cracking (FCC), circulating fluidized bed combustion (CFBC), coal gasification, and sulfide roasting. Earlier studies of these systems mainly focused on experimental investigations including measurement of macroscopic hydrodynamic behavior and development of some corresponding correlations. In recent decades, to quantitatively understand the complex hydrodynamics of gas-solid fluidization, the computational fluid dynamics approach is adopted in many cases, and a lot of numerical methods in the hydrodynamic modeling and simulation of gas-solid fluidization have been proposed, such as two-fluid model (TFM) (Anderson and Jackson, 1967; Ishii, 1975), quadrature-based moment methods (QBMM) (Fox, 2008, 2009a,b; Desjardins et al., 2008;), discrete particle simulation (DPS) (Tsuji et al., 1993; Hoomans et al., 1996; Xu and Yu, 1997), and direct numerical simulation (DNS) (Hu et al., 1992; Ma et al., 2006; Wang et al., 2010; Xiong et al., 2012).

Among these numerical methods, the most frequently used TFM treats the gas and solid phases as two interpenetrating continua, and locally averaged quantities such as volume fractions, velocities, species concentrations, and temperatures of gas and solid phases appear as dependent field variables (Anderson and Jackson, 1967; Ishii, 1975). To derive TFM using ensemble averaging techniques, terms such as effective stresses and the inter-phase interaction have to be introduced, which require constitutive equations for closure. Only under very limited conditions, those constitutive equations can be obtained rigorously from the kinetic theory of granular flow (Gidaspow, 1994), otherwise we have to resort to empirical models. The accuracy and effectiveness of TFM are, therefore, still unsatisfactory in many circumstances. The recently developed QBMM permits to solve population balance equation (PBE) in commercial CFD codes at relatively low computational cost. However, its application to the context of multiphase flows is to be explored (Mazzei, 2011). Comparably, DNS not only fully resolves the motion of each individual solid particle and fluid flow, but also directly calculates the hydrodynamic force acting on each individual solid particle from the stress on the fluid-solid boundary. Due to its capability in detailed solution around each particle, DNS has been regarded as the most accurate method for the simulation of gas-solid flow. Unfortunately, DNS is too costly for predicting the hydrodynamics in large industrial scale fluidized beds even at low Reynolds numbers, let alone the high Reynolds number cases where their grid size and time step are

* Corresponding author. Tel.: +86 10 8254 4942; fax: +86 10 6255 8065.
Email address: lmwang@home.ipe.ac.cn (Limin Wang)

limited by the Kolmogorov length scale and the turbulence time scale (Xiong et al., 2012).

For numerical modeling of gas-solid fluidized beds mentioned above, TFM is computationally more economic but inaccurate, while DNS is computationally more accurate but expensive. So it is natural to ask whether there exists a better alternative combining the advantages of the two methods for modeling the gas-solid flows. As a particle-scale approach, DPS is somehow in between these two ends and seems to give a good balance among accuracy, cost and efficiency. Specifically, DPS resolves the continuum fluid flow at the scale of computational cells in CFD, describes the motion of individual particles by the well-established Newton's equations of motion, and models particle-particle interactions through different collision models such as the hard-sphere model and the soft-sphere model, which has been proven to be effective in modeling various particle flow systems (Deen et al., 2007; Zhu et al., 2007, 2008), such as slugging fluidized bed (Xu et al., 2007), spouted bed (Zhao et al., 2008), pneumatic conveying (Kuang et al., 2008), bubbling fluidized bed (Geng and Che, 2011), sound-assisted fluidized bed (Wang et al., 2011), and cyclone separator (Chu et al., 2011). However, in all these mentioned work, the fluid motion with suspended solids is commonly governed by the volume-averaged Navier-Stokes equations or their simplified forms (Tsuji et al., 1993; Hoomans et al., 1996; Xu and Yu, 1997; Mikami et al., 1998), and those equations are solved based on implicit schemes no matter by Fluent (Chu and Yu, 2008a, b; Chu et al., 2009a, b, 2011; Wu et al., 2010; Zhao et al., 2010), OpenFOAM (Su et al., 2011; Goniva et al., 2012), MFIX (Darabi et al., 2011; Garg et al., 2012; Li and Guenther, 2012; Li et al., 2012a,b; Gopalakrishnan and Tafti, 2013), or in-house codes (Ouyang and Li, 1999a, b; Zhou et al., 2004a, b; Zhao et al., 2009; Wang et al., 2009; Wu et al., 2009). With implicit methods the discretized equations are solved simultaneously which inevitably requires some kind of global data dependence and hence global communication. Therefore, most algorithms involved suffer from relatively lower scalability and parallel efficiency, which becomes a grand challenge for fast simulation of large-scale industrial systems.

As a smoothed alternative to lattice gas automata (LGA), lattice Boltzmann method (LBM) (McNamara and Zanetti, 1988) is an efficient second-order flow solver capable of solving various systems for hydrodynamics owing to its explicit solution of particle distribution function, algorithmic simplicity, natural parallelism, and flexibility in boundary treatment (Chen and Doolen, 2003). Therefore, LBM becomes an increasingly popular approach to simulation of complex flows (Aidun and Clausen, 2010) and can be easily incorporated into DPS. Filippova and Hanel (1997) proposed a combination of lattice-BGK model and Lagrangian approach, and performed three-dimensional simulation of gas-particle flow through filters with one-way coupling, where the fluid affected the particles but the particles did not affect the fluid. Chen et al. (2004) simulated particle-laden flow over a backward-facing step with two-way coupling, where a modified lattice-BGK model was developed for the fluid flow and a Lagrangian approach for particles. But they did not consider the effect of solid volume

fraction on gas flows. Sungkorn et al. (2011) proposed a gas-liquid Lagrangian-LBM to simulate turbulent gas-liquid bubbly flows with a relatively low gas holdup. Specifically, they solved the continuous liquid phase by single-phase lattice Boltzmann equation (LBE) incorporated with large eddy simulation (LES) (Smagorinsky, 1963), and evolved the dispersed gas phase (i.e. the individual bubbles) by Lagrangian trajectories, but did not include the gas volume fraction in the conservation equations and its effect on drag force.

In this paper, we proposed a modified LBE to model the fluid flow and developed the corresponding fluid-solid interaction model in the framework of DPS. The effects of both the local solid volume fraction and the local relative velocity between particles and fluid are considered. The equations of motion governing individual particles are solved with time-driven hard-sphere (TDHS) model. It is noteworthy that the computational strategy herein has ever been implemented in direct simulation of particle-fluid systems (Wang et al., 2010) where the modified LBE was used with particle size much larger than the cell spacing. In the present work, the partial saturation concept has been extended to model the objects much smaller than the cell spacing (i.e. porous media), and both the linear and nonlinear drag effects of the solid phase (media) have been considered in the lattice Boltzmann based discrete particle simulation for the first time.

2. Numerical approach

The objective of this research is to develop a lattice Boltzmann based numerical method for discrete simulation of gas-solid fluidization systems. For illustration, we used two-dimensional nine-velocity (D2Q9) lattice Boltzmann model as an example, and the solid particles distributed in the lattice cell are described by the time-driven hard sphere model. A schematic diagram of this method is shown as Fig. 1.

2.1. LBM for gas phase hydrodynamics

The particle distribution function $f(t, \mathbf{x}, \mathbf{v})$ is the number of particles per unit volume with velocity \mathbf{v} at time t and position \mathbf{x} , which is often used in non-equilibrium statistical mechanics. The evolution of the distribution function f is described by the Boltzmann equation (Chapman and Cowling, 1970):

$$\frac{\partial f(t, \mathbf{x}, \mathbf{v})}{\partial t} + \mathbf{v} \cdot \frac{\partial f(t, \mathbf{x}, \mathbf{v})}{\partial \mathbf{x}} = \Omega \quad (1)$$

The left-hand side of this equation is an advection term, while the right-hand side contains the collision operator Ω which describes the interaction between particles. External forces are neglected in this derivation. After a finite difference discretization of the Boltzmann equation in time, space and velocity, LBE is simplified as (McNamara and Zanetti, 1988),

$$f_i(\mathbf{x} + \mathbf{c}_i \Delta t, t + \Delta t) - f_i(\mathbf{x}, t) = \Omega_i \quad (2)$$

where the subscript i represents the orthogonal and diagonal directions in the Cartesian coordinates, f_i is the particle distribution function in direction i , \mathbf{c}_i is the discrete velocity in direction

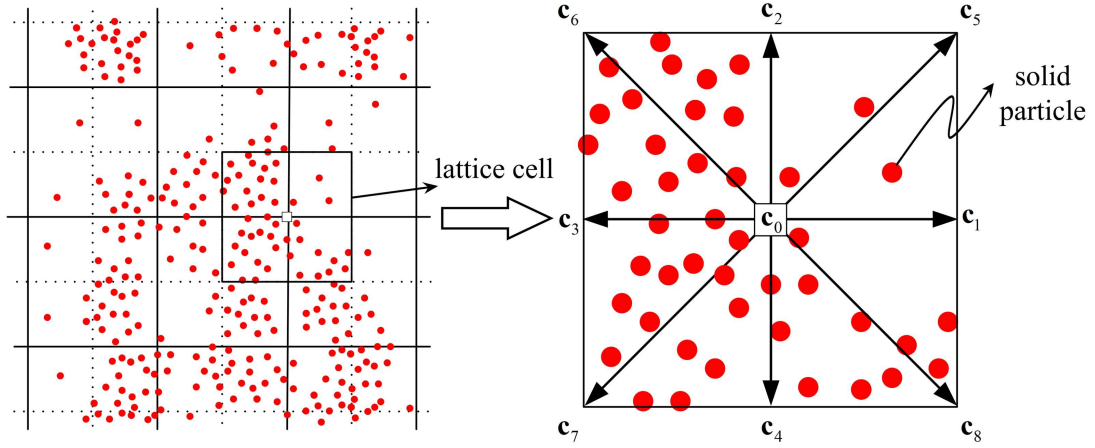


Figure 1: The schematic diagram of D2Q9 computational fluid lattices and solid particles.

i , \mathbf{x} and t are the lattice simulation position and time, respectively, and Ω_i is collision term in direction i . Assuming that the collision frequency is a function of spatial coordinates and time, and independent of the molecular velocity, the collision term Ω_i can be approximated by the so-called BGK (Bhatnagar et al., 1954) model:

$$\Omega_i = -\frac{\Delta t}{\tau} (f_i - f_i^{\text{eq}}) \quad (3)$$

Here $\tau = 3\nu + \frac{\Delta t}{2}$ is the relaxation time related to kinematic viscosity and the discrete time step Δt , f_i^{eq} is the equilibrium distribution function expressed as (Qian et al., 1992)

$$f_i^{\text{eq}}(\rho, \mathbf{u}) = \omega_i \rho \left(1 + \frac{\mathbf{c}_i \cdot \mathbf{u}}{c_s^2} + \frac{(\mathbf{c}_i \cdot \mathbf{u})^2}{2c_s^4} - \frac{\mathbf{u} \cdot \mathbf{u}}{2c_s^2} \right) \quad (4)$$

where \mathbf{c}_i is defined as $\mathbf{c}_i = \{\cos[(i-1)\pi/2], \sin[(i-1)\pi/2]\}$ for $i = 1 \sim 4$ and $\mathbf{c}_i = \sqrt{2} \{\cos[(i-5)\pi/2], \sin[(i-5)\pi/2]\}$ for $i = 5 \sim 8$, and $\mathbf{c}_0 = 0$. The weights are given by $\omega_0 = 4/9$, $\omega_i = 1/9$ for $i = 1 \sim 4$, $\omega_i = 1/36$ for $i = 5 \sim 8$, and c_s is the speed of sound and equals to $\sqrt{3}/3$ in lattice unit, ρ and \mathbf{u} are density and velocity, respectively.

The macroscopic quantities such as mass density and momentum density can then be obtained by evaluating the hydrodynamic moments of the distribution function $f_i(\mathbf{x}, t)$, namely,

$$\rho = \sum_{i=0}^8 f_i \quad \text{and} \quad \rho \mathbf{u} = \sum_{i=0}^8 \mathbf{c}_i f_i \quad (5)$$

By the Chapman-Enskog procedure (Sterling and Chen, 1996; Guo et al., 2002), the incompressible Navier-Stokes equations can be obtained from LBE in the limit of small Mach number. Therefore, the standard LBE is just suitable for single-phase flow. To model incompressible gas flow through suspended particles, an immersed moving boundary method for a medium with porosity needs to be introduced in LBM framework.

The key idea of the immersed moving boundary method is that the effect of boundary is modeled using a source term in the

momentum equations. Here, the particle-fluid coupling is implemented by immersed moving boundary method (Noble and Torczynski, 1998; Cook et al., 2004), which introduces a term that depends on the percentage of the cell saturated with fluid to modify the collision operator and represent the effect of both the solid volume fraction and the gas-solid slip velocity on hydrodynamics. Although most of applications of the immersed moving boundary are associated with the objects whose size is much larger than the cell spacing (Noble and Torczynski, 1998; Cook et al., 2004; Feng et al., 2007; Wang et al., 2010; Zhou et al., 2011; Xiong et al., 2012; Wei et al., 2013), the method is theoretically not confined to this scale. Therefore, the partial saturation concept is extended to model the objects with much smaller size than the cell spacing, and the corresponding LBE modified for partially saturated cells (Noble and Torczynski, 1998) reads

$$f_i(\mathbf{x} + \mathbf{c}_i \Delta t, t + \Delta t) = f_i(\mathbf{x}, t) - \frac{1}{\tau} (1 - \gamma(\varepsilon_s, \tau)) (f_i(\mathbf{x}, t) - f_i^{\text{eq}}(\mathbf{x}, t)) + \gamma(\varepsilon_s, \tau) \Omega_i^s \quad (6)$$

where Ω_i^s is an additional collision term that accounts for the bounce back of the non-equilibrium part of the distribution function, and Ω_i^s is given by (Noble and Torczynski, 1998)

$$\Omega_i^s = f_{-i}(\mathbf{x}, t) - f_i(\mathbf{x}, t) + f_i^{\text{eq}}(\rho, \mathbf{v}_s) - f_{-i}^{\text{eq}}(\rho, \mathbf{u}) \quad (7)$$

where $-i$ denotes the component of the distribution function opposite to i and \mathbf{v}_s is the average velocity of solid phase at the computational lattice. \mathbf{v}_s can be approximately calculated as

$$\mathbf{v}_s = \frac{\sum_{k=1}^{n_{\text{tot}}} \mathbf{v}_k}{n_{\text{tot}}} \quad (8)$$

where \mathbf{v}_k is the velocity of solid particle k and n_{tot} is the number of solid particles in fluid cell (see Fig.1).

The weighting function γ in Eq. (6) depends on the relaxation time τ and the solid volume fraction ε_s of each cell, which is given, among other forms, by (Noble and Torczynski, 1998)

$$\gamma(\varepsilon_s, \tau) = \frac{\varepsilon_s(\tau - 0.5)}{(1 - \varepsilon_s) + (\tau - 0.5)} \quad (9)$$

In our case, since the gas velocity \mathbf{u} presents a spatial average over areas fully, partially or not occupied by the solid phase, a different expression of γ may be developed. But as a rough estimation, we will at first neglect the actual difference of gas velocity at different locations within each lattice and continue to use the expression of Eq. (9). Obviously, $\gamma = 0$ and $\gamma = 1$ represent pure fluid and pure solid states, respectively.

The solid volume fraction ε_s is related to the porosity of lattice cell ε_{2d} , namely $\varepsilon_{2d} = 1 - \varepsilon_s$. ε_{2d} , an important parameter that influences both the gas-phase and solid-phase motions, can be calculated based on the area occupied by the particles in the lattice cell. The two-dimensional porosity of solid phase is given by

$$\varepsilon_{2d} = 1 - \frac{n_{\text{tot}} \cdot \pi r^2}{h^2} \quad (10)$$

where r is the radius of solid particle and h is lattice spacing between nodes. As the drag-force correlation is based on 3D systems, we also use a 3D porosity transformed from 2D porosity for this purpose. According to (Ouyang and Li, 1999a),

$$\varepsilon_{3d} = 1 - \frac{\sqrt{2}}{\sqrt{\pi \sqrt{3}}} (1 - \varepsilon_{2d})^{3/2} \quad (11)$$

To capture turbulent structures in gas-solid fluidization systems which are usually associated with large Reynolds numbers or become turbulent in nature, meso-scale turbulence models are incorporated into the volume-averaged Navier-Stokes equations in DPS (Zhou et al., 2004a, b; Gui et al. 2008; Liu and Lu, 2009), here LES incorporated into LBM is used (Krafczyk et al., 2003; Yu et al., 2005). The effect of the small sub-grid eddies on the large-scale flow structures are modeled through an additional turbulent viscosity ν_e .

In Smagorinsky-based subgrid scale (SGS) model (Smagorinsky, 1963), ν_e depends on the strain rate:

$$\nu_e = (C_s \Delta x)^2 \|S\|, \quad S = \sqrt{2S_{ij}S_{ij}} \quad (12)$$

Here C_s is the Smagorinsky constant and strain rate tensor $S_{ij} = (\partial_j u_i + \partial_i u_j)/2$ can be obtained directly by computing the momentum fluxes Q_{ij} , which are second-order moments of the non-equilibrium distribution function (Yu et al., 2005):

$$S_{ij} = \frac{1}{2\rho c_s^2 \tau} Q_{ij}, \quad Q_{ij} = \sum_{k=0}^8 c_{ki} c_{kj} (f_k - f_k^{\text{eq}}) \quad (13)$$

$$S = \frac{Q}{2\rho c_s^2 \tau_t}, \quad Q = \sqrt{2Q_{ij}Q_{ij}}$$

where c_{ik} is the k th component of the lattice velocity \mathbf{c}_i . Based on an eddy relaxation time assumption for sub-grid scale stress, the effect of the flow structure at the unresolved scale is modeled through an effective collision relaxation time τ_e , which is the eddy relaxation time with respect to the eddy viscosity ν_e . The eddy viscosity is then incorporated into the LBE by using $\tau_t = \tau + \tau_e$ instead of τ in Eq. (6). Accordingly,

$$\tau_t = \frac{3}{c^2} \nu_t + \frac{1}{2} \Delta t = \frac{3}{c^2} (\nu + \nu_e) + \frac{1}{2} \Delta t \quad (14)$$

where c is the lattice speed given by $h/\Delta t$. From Eq. (13) and Eq. (14), a quadratic equation is obtained, which yields

$$\tau_t = \tau + \tau_e = \frac{1}{2} \left(\tau + \sqrt{\tau^2 + 18C_s^2 (\Delta x)^2 Q} \right) \quad (15)$$

It should be pointed out that Eq. (15) is suitable for both laminar and turbulent flows. On the one hand, under high gas velocity, Q is large and hence $\tau_t \gg \tau$, which expresses the effect of motion at unresolved scale. On the other hand, under low gas velocity, Q vanishes and $\tau_t \approx \tau$, describing the laminar flow.

2.2. TDHS for particle dynamics

Each individual solid particle, treated as a point-volume particle, has four properties: mass (m), radius (r), position (\mathbf{P}), and velocity (\mathbf{v}). According to Newton's second law of motion, the equation of motion for solid particle k is

$$m \frac{d\mathbf{v}_k}{dt} = m\mathbf{g} + (\mathbf{F}_d)_k + (\mathbf{F}_c)_k + (V_p)_k \nabla p_k \quad (16)$$

where \mathbf{g} is the gravitational acceleration, $(\mathbf{F}_d)_k$ is the drag force, $(\mathbf{F}_c)_k$ is the collision force, $(V_p)_k$ is the particle's volume, and ∇p_k is the pressure gradient.

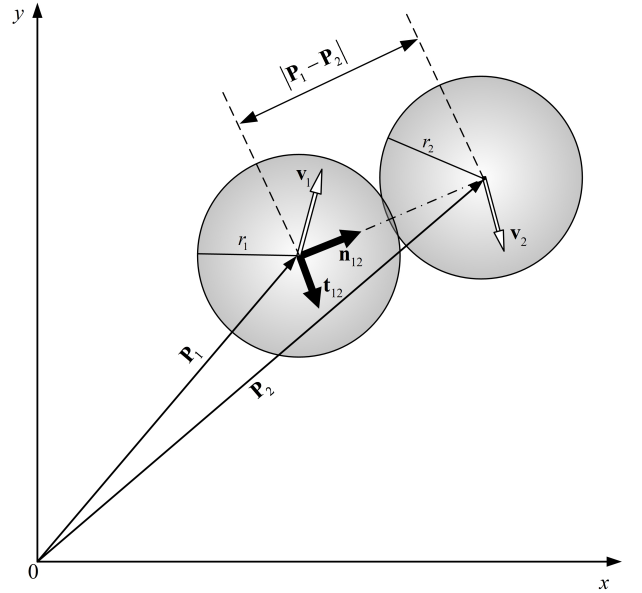


Figure 2: The schematic illustration of two colliding particles.

Time-driven hard-sphere model (Hopkins and Louge, 1991) is used for particle-particle collisions; while particles interact as binary and quasi-instantaneous hard-spheres, and both the collisions are detected and the particle state are updated at constant time intervals. Namely, when two particles are in contact with each other and if the internal product of $\mathbf{P}_1 - \mathbf{P}_2$ and $\mathbf{v}_1 - \mathbf{v}_2$ is negative, which means that the particles are moving closer to each other, they will collide (see Fig. 2). For the collision between particle 1 and particle 2, the post-collisions velocities can be obtained by the following formulae:

$$\mathbf{v}_1^* = \mathbf{v}_1 - \frac{(1+e)m_2}{m_1+m_2} \frac{(\mathbf{v}_1 - \mathbf{v}_2) \cdot (\mathbf{P}_1 - \mathbf{P}_2)}{|\mathbf{P}_1 - \mathbf{P}_2|^2} (\mathbf{P}_1 - \mathbf{P}_2) \quad (17)$$

$$\mathbf{v}_2^* = \mathbf{v}_2 + \frac{(1+e)m_1(\mathbf{v}_1 - \mathbf{v}_2) \cdot (\mathbf{P}_1 - \mathbf{P}_2)}{m_1 + m_2} \frac{(\mathbf{P}_1 - \mathbf{P}_2)}{|\mathbf{P}_1 - \mathbf{P}_2|^2} \quad (18)$$

where “*” means post-collision velocities, e is the restitution coefficient that represents the ratio of speeds after (post-) and before (pre-) collision, and the velocities in the right-hand side of the equations are pre-collision velocities. The walls involved in simulations are composed of infinitely heavy particles with zero velocity, and the collisions between particles and the wall also satisfy Eqs. (17) and (18). In the next time step, the particles move to new positions with their new velocities.

It should also be noted that particle-particle interactions are important in simulating gas-solid fluidization, especially for dense gas-fluidized beds. In time-driven hard-sphere model mentioned above, only the binary-particle collision mechanism and the normal component of contact force are considered, which limits the model to low solid holdup conditions (less than 30~40% by volume). For dense gas-fluidized beds, discrete element method (DEM) (Cundall and Strack, 1979) might be expected to reflect both the multi-particle collision mechanism and the tangential component of contact force.

2.3. Inter-phase momentum transfer

The drag correlations are of great importance in numerical models that predict the flow behavior of gas-solid fluidized beds. The inter-phase momentum transfer coefficient based on the traditional Ergun and Wen & Yu correlations (Gidaspow, 1994; Gidaspow and Jiradilok., 2009) is only valid for homogeneous particle suspensions, and insufficient to capture the heterogeneous structures of gas-solid fluidization. A structure-dependent drag based on the energy minimization multi-scale model (EMMS) is used here, that is (Yang et al., 2003)

$$\beta = \begin{cases} \frac{3}{4} \frac{(1 - \varepsilon_g) \varepsilon_g \rho_g |\mathbf{u} - \mathbf{v}|}{d_p} C_{d0} \cdot \omega, & \varepsilon_g > 0.74, \\ 150 \frac{(1 - \varepsilon_g)^2 \mu_g}{\varepsilon_g d_p^2} + 1.75 \frac{(1 - \varepsilon_g) \rho_g |\mathbf{u} - \mathbf{v}|}{d_p}, & \varepsilon_g \leq 0.74. \end{cases} \quad (19)$$

According to Yang et al. (2003), the drag correction factor

$$\omega = \begin{cases} \frac{0.0214}{4(\varepsilon_g - 0.7463)^2 + 0.0044} - 0.5760, & 0.74 < \varepsilon_g \leq 0.82, \\ \frac{0.0038}{4(\varepsilon_g - 0.7789)^2 + 0.0040} - 0.0101, & 0.82 < \varepsilon_g \leq 0.97, \\ 32.8295\varepsilon_g - 31.8295, & \varepsilon_g > 0.97. \end{cases} \quad (20)$$

The drag coefficient C_{d0} for isolated rigid spherical particle can be calculated by the Schiller and Nauman (1935) equation

$$C_{d0} = \begin{cases} \frac{24}{Re_p} (1 + 0.15Re_p^{0.687}), & Re_p < 1000, \\ 0.44, & Re_p \geq 1000. \end{cases} \quad (21)$$

Here the particle Reynolds number is defined as follows:

$$Re_p = \frac{\varepsilon_g \rho_g |\mathbf{u} - \mathbf{v}| d_p}{\mu_g} \quad (22)$$

It has been demonstrated that the drag correction factor ω , varying in value between 0.0152 and 4.2876, plays an important role in simulation of gas-solid fluidization (Yang et al., 2003), and hence is employed in a similar way to reflect the heterogeneous structures. The modified LBE is thus written as

$$f_i(\mathbf{x} + \mathbf{c}_i \Delta t, t + \Delta t) = f_i(\mathbf{x}, t) - \frac{1}{\tau_t} (1 - \gamma(\varepsilon_s, \tau_t)) (f_i(\mathbf{x}, t) - f_i^{\text{eq}}(\mathbf{x}, t)) + \omega \gamma(\varepsilon_s, \tau) \Omega_i^s \quad (23)$$

Accordingly, the volume-averaged gas velocity must be re-defined as (Guo and Zhao, 2002; Guo et al., 2002)

$$\rho \mathbf{u} = \sum_{i=0}^8 \mathbf{c}_i \left(f_i + \frac{1}{2} \omega \gamma \Omega_i^s \right) \quad (24)$$

It should be stressed here that the gas velocity calculated from the modified LBE is the superficial gas velocity and needs to be converted into the actual gas velocity.

The hydrodynamic force acting on the fluid in a computational cell, $\mathbf{F}_{p \rightarrow g}$, can be calculated by summing up the momentum transfer that occurs in all discrete directions as

$$\mathbf{F}_{p \rightarrow g} = \frac{h^2}{\Delta t} \omega \gamma \sum_{i=0}^8 \Omega_i^s \mathbf{c}_i \quad (25)$$

Then a pre-estimated drag force acting on solid particle k , $(\mathbf{F}_d)_k^{\text{pre}}$, can be calculated according to the following equation (Hoomans et al., 1996; Li and Kuipers, 2003):

$$(\mathbf{F}_d)_k^{\text{pre}} = \frac{(V_p)_k \beta_k}{1 - \varepsilon_k} (\mathbf{u}_k - \mathbf{v}_k) \quad (26)$$

Here the local inter-phase momentum transfer coefficient β_k , the local gas velocity \mathbf{u}_k and the local voidage ε_k are all calculated by bilinear interpolation using the values of four surrounding grid nodes. In each computational cell (see Fig. 3), the pre-estimated total drag force acting on all the particles, $\mathbf{F}_{g \rightarrow p}^{\text{pre}}$, can be obtained as

$$\mathbf{F}_{g \rightarrow p}^{\text{pre}} = \sum_{k=1}^{n_{\text{tot}}} (\mathbf{F}_d)_k^{\text{pre}} \quad (27)$$

which is not necessarily equal to the hydrodynamic force acting on the fluid. To satisfy Newton's third law, the pre-estimated drag force acting on solid particle k , $(\mathbf{F}_d)_k^{\text{pre}}$, is then adjusted to

$$\begin{aligned} (F_d)_k^x &= \frac{|F_{p \rightarrow g}^x|}{|F_{g \rightarrow p}^{\text{pre}, x}|} \frac{(V_p)_k \beta_k}{1 - \varepsilon_k} (u_k^x - v_k^x), \\ (F_d)_k^y &= \frac{|F_{p \rightarrow g}^y|}{|F_{g \rightarrow p}^{\text{pre}, y}|} \frac{(V_p)_k \beta_k}{1 - \varepsilon_k} (u_k^y - v_k^y) \end{aligned} \quad (28)$$

where $(F_d)_k^x$ and $(F_d)_k^y$ are the x- and y-components of the drag force acting on solid particle $(\mathbf{F}_d)_k$, respectively. The total drag force acting on all the particles, $\mathbf{F}_{g \rightarrow p}$, can be obtained

$$\mathbf{F}_{g \rightarrow p} = \sum_{k=1}^{n_{\text{tot}}} (\mathbf{F}_d)_k \quad (29)$$

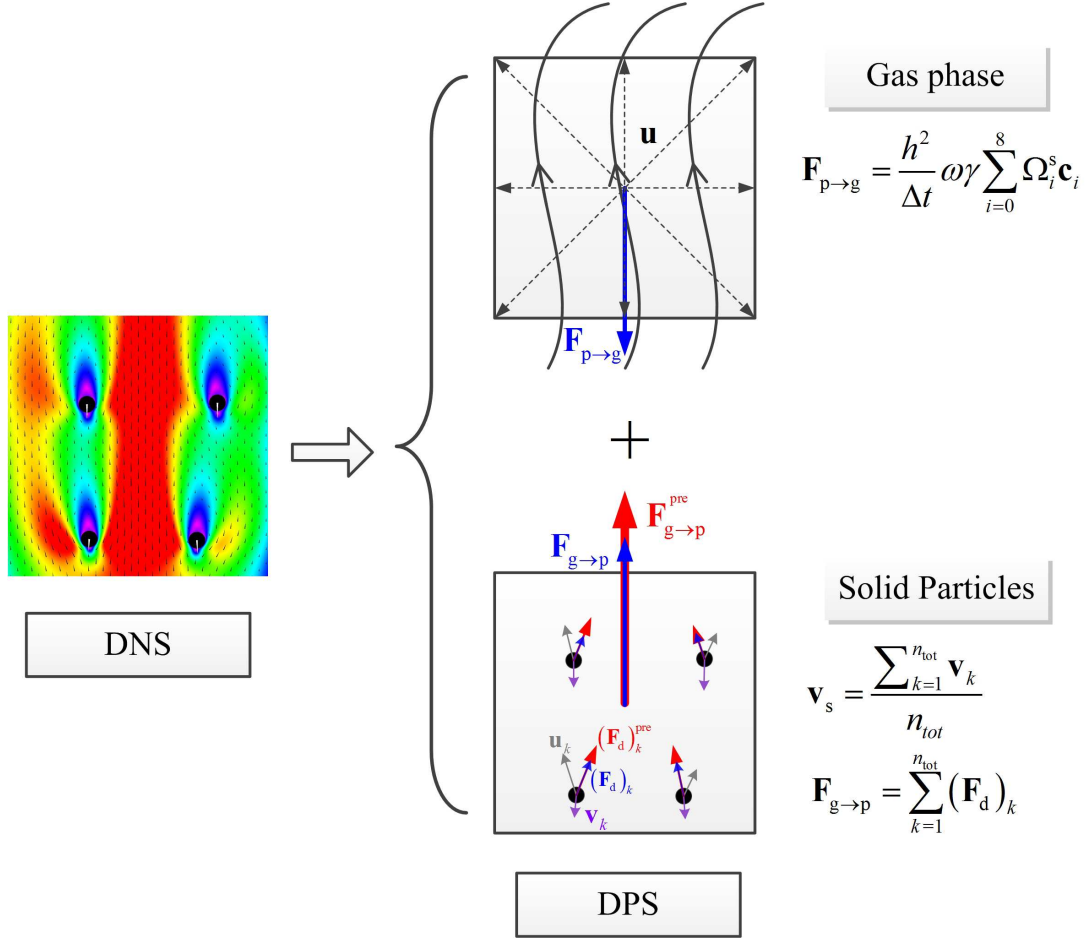


Figure 3: The schematic diagram of gas-solid coupling and drag force correction in a computational cell.

With this drag force correction, the value of the total drag force acting on all the particles automatically equals to the value of the hydrodynamic force acting on the fluid in each computational cell and the Newton's third law, $\mathbf{F}_{g \rightarrow p} = \mathbf{F}_{p \rightarrow g}$, is also automatically satisfied in Eqs. (24) and (29).

2.4. Computational algorithm and implementation

In traditional DPS, the drag force acting on an individual solid particle is first calculated by the empirical formula Eq. (26), then the total drag force acting on all the particles in each computational cell is calculated by Eq. (27), and the total drag force, as a source term of force, is added into the momentum equation for the fluid phase, which is finally solved to obtain the fluid phase velocity field.

The procedure in this work is slightly different from the case that the fluid phase velocity field is first obtained from the evolution of the modified LBE, the total drag force acting on all the particles is simultaneously calculated by Eq. (25), and then the total drag force is distributed to each particle in the computational cell with the corrections described in Eqs. (26)~(28). In fact, the pre-estimated drag force acting on the solid particles plays the role of a weight function for this distribution. The step-by-step procedure for the lattice Boltzmann based discrete

simulation is outlined in Fig.4, which mainly includes the following steps:

- 1) Input the initial data such as the size and geometry of the simulation domain (for both the solid and fluid phases), the specified boundary conditions (i.e. particle distribution, initial flow field, velocity profile, etc.). The wall boundary condition given in this paper is the bounce-back scheme for fluid and specular reflections for solid particles (Wang et al., 2006).
- 2) Perform the statistical calculations of the average velocity and the porosity of solid phase at the fluid lattice nodes according to Eq. (8) and Eq. (11), respectively.
- 3) Perform the consecutive propagation and collision process over a discrete fluid lattice cell, and then evolve the fluid flow according to the modified LBE (Eq. (23)), finally obtain the gas flow field and pressure filed.
- 4) The local gas velocities, the local pressure gradient, the local porosity, and the local inter-phase momentum transfer coefficient at the center of the particle are calculated by bilinear interpolation using the values of the surrounding computational lattices. Compute $\mathbf{F}_{p \rightarrow g}$ from Eq. (25) and $\mathbf{F}_{g \rightarrow p}^{pre}$ from Eqs. (26) and (27) at all lattice nodes. Substitute these values of $\mathbf{F}_{p \rightarrow g}$ and $\mathbf{F}_{g \rightarrow p}^{pre}$ into Eq. (28), obtain the drag force acting on the each particle $(\mathbf{F}_d)_k$.

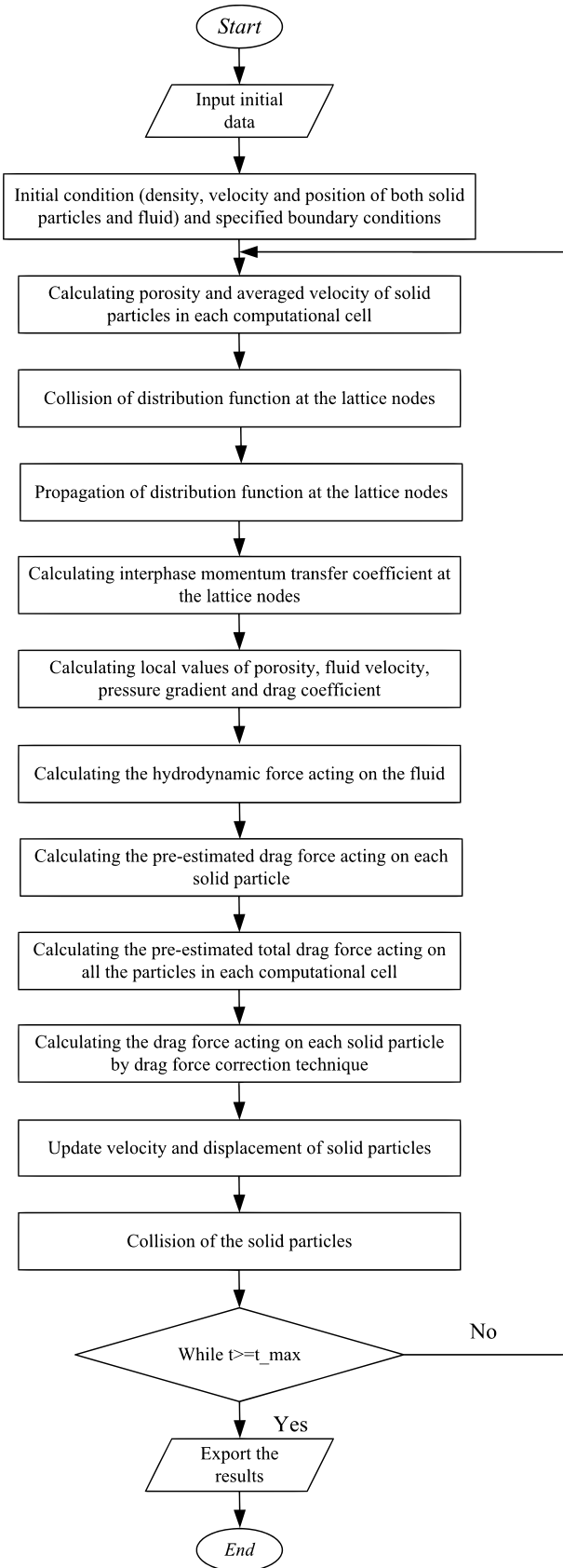


Figure 4: The flow chart of lattice Boltzmann based discrete particle simulation.

- 5) Integrate the particle motion equation (Eq. (16)) numerically to calculate the velocities and the trajectories of individual particles.
- 6) Detect the instantaneous collisions of solid particles according to new particle positions and velocities. If the instantaneous collisions occur, the post-collision velocities of individual particles are determined according to Eqs. (17) and (18).
- 7) Evolve the next time and go back to step 2 unless the set time step is reached.

3. Simulations and results

To validate the proposed model, two typical fluidization processes, namely, a single bubble injected into a fluidized bed at incipient fluidization condition and particle clustering in the riser of a circulating fluidization bed, are simulated and compared with published correlations and experimental data. To simplify the simulation, the gas weight is neglected, but the effective gravity acting on the particles is corrected as $(1.0 - \rho_g/\rho_s)\mathbf{g}$.

3.1. A single bubble injected into a fluidized bed at incipient fluidization

In this example, a pulse of gas is injected at the bottom of a fluidized bed at incipient fluidization, the gas velocity on both sides of the central orifice is set as the minimum fluidization velocity (background gas velocity) v_{mf} , and the injection lasts 0.006 seconds. The parameters used for the simulation are summarized in Table 1.

Figure 5 presents the snapshots of bubble formation at different times. We observe the growth of the spherical cap bubble from an initially small perturbation in the bulk of the bed (see Fig. 5(a)~(e)) to its subsequent detachment and rising (see Fig. 5(f)~(h)). Eventually, the bubble wake is followed when the kidney-bubble detaches from the bottom of the bed (see Fig. 5(j)~(n)). Finally, the bubbles arrive at the surface, and it lifts some particles from wake into the bubble and causes the break-up of the bubble (see Fig. 5(o)~(p)). This phenomenon is in qualitative agreement with the previous simulation and experimental results of bubbling (Rowe and Yacono, 1976; Nieuwland et al., 1996). It should be noted that the rising bubble shape is more spherical-cap than the elliptic bubble shape in the experimental and numerical results of Bokkers et al. (2004) due to the smaller solid particle diameter.

Figure 6 shows that the gas phase leaves the roof of bubble, and the downward moving particles near the wall drag the gas to the bottom of the bubble where it re-enters the bubble region, resulting in a pair of symmetrical vortices which are observed in the neighborhood of the rising bubble. In addition, the simulated fluidizing gas streamlines passing through a rising bubble are close to those predicted by the two-phase model of a fluidized bed (Davidson and Harrison, 1963). These results illustrate that the modified LBE is capable of capturing accurately the detailed flow structure of the gas phase.

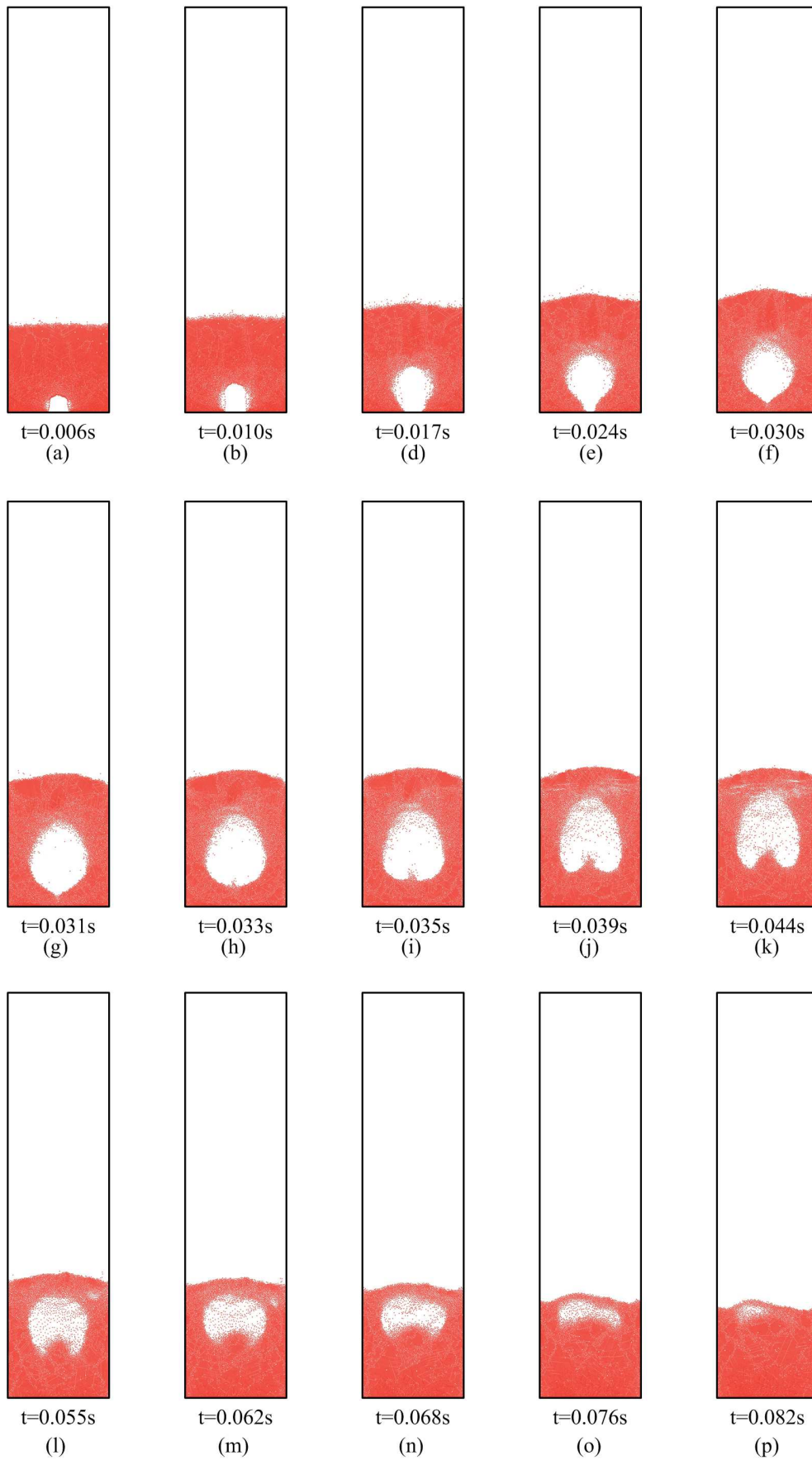


Figure 5: Evolution of bubble formation at a single orifice.

Table 1: Simulation and physical parameters used for bubbling simulation

Item	Dimensional	Dimensionless
Bed width W (m)	0.00675	25
Bed height H (m)	0.027	100
Orifice width r_{inj} (m)	0.00081	3
Solid particle diameter d_p (m)	5.4×10^{-5}	0.2
Cell or lattice size h (m)	2.7×10^{-4}	1
Time step t (s)	1.35×10^{-6}	1
Minimum fluidization velocity v_{mf} (m/s)	0.0025	1.25×10^{-5}
Injection velocity v_{inj} (m/s)	0.8	0.04
Gas density ρ_g (kg/m ³)	1.1795	1
Solid density ρ_s (kg/m ³)	930.0	788.5
Gas viscosity μ_g (kg/(m·s))	1.8872×10^{-5}	2.96×10^{-4}
Coefficient of restitution e	0.9	0.9
Particle number N	15000	15000

The volume-averaged equivalent bubble diameter is defined as the diameter of a circle with equal area to the region where the gas voidage is higher than 0.85 (Nieuwland et al., 1996). The computed maximum bubble diameter D_e at different injection velocities is shown in Fig. 7, together with the correlations of Cai et al. (1994). The results show that D_e increases with the increasing of injection velocities (or equivalently overall superficial gas velocity), and the deviation is below 5%, suggesting that the simulation results are reasonable.

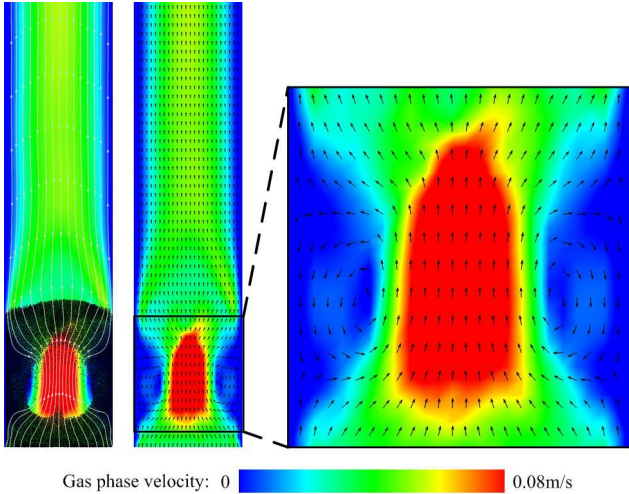


Figure 6: Snapshots of the flow field of gas phase at simulation time $t=0.035s$.

3.2. Riser behavior of fluidization systems

The riser hydrodynamics of circulating fluidized beds (CFB) have been investigated extensively in both experiments and simulations in past decades. Our simulation refers to a CFB estab-

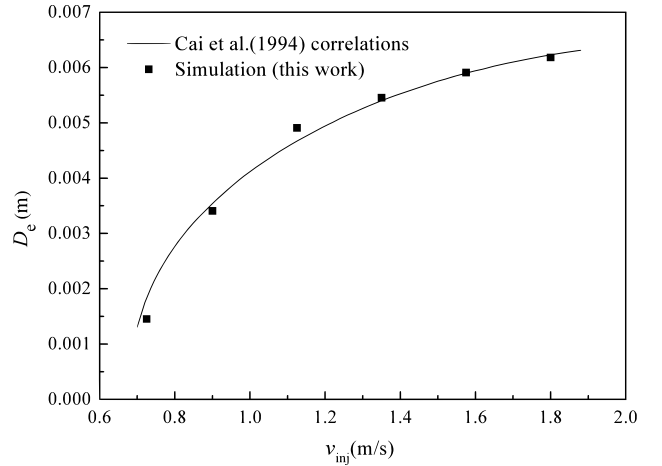


Figure 7: Comparison of the correlation formula (Cai et al., 1994) obtained and simulated maximum bubble diameter for a range of injection velocities.

lished by Li and Kwauk (1994), for which a large number of experimental data have been collected. The 2D riser configuration has been reported enough to mimic the real system (Camarata et al., 2003; Xie et al., 2008), and the comparison of planar 2D simulation results with cylindrical 3D experimental data could also be found widely in the literature to study gas-solid fluidized beds (Wang et al., 2008; Lan et al., 2009; Lu et al., 2011; Chen et al., 2012; Li et al., 2012). Table 2 lists the parameters used in this present simulation.

Figure 8 shows some snapshots from this simulation. Apparently, radial and axial heterogeneous structures are formed spontaneously and gradually from the homogeneous initial state and appear all the time hereafter.

Figure 9 shows the evolution of the simulated solids flux with time and its comparison with experimental data of Li

Table 2: Simulation and physical parameters used for riser of circulating fluidized beds

Item	Dimensional	Dimensionless
Bed width W (m)	0.0162	60
Bed height H (m)	0.194	720
Initial solids volume fraction θ_s	0.09007	0.09007
Solid particle diameter d_p (m)	5.4×10^{-5}	0.2
Cell or lattice size h (m)	2.7×10^{-4}	1
Time step t (s)	6.0×10^{-6}	1
Gas velocity at the inlet v_{inlet} (m/s)	1.52	0.0338
Gas density ρ_g (kg/m ³)	1.1795	1
Solid density ρ_s (kg/m ³)	930.0	788.5
Gas viscosity μ_g (kg/(ms))	1.8872×10^{-5}	1.32×10^{-4}
Coefficient of restitution e	0.9	0.9
Particle number N	123921	123921

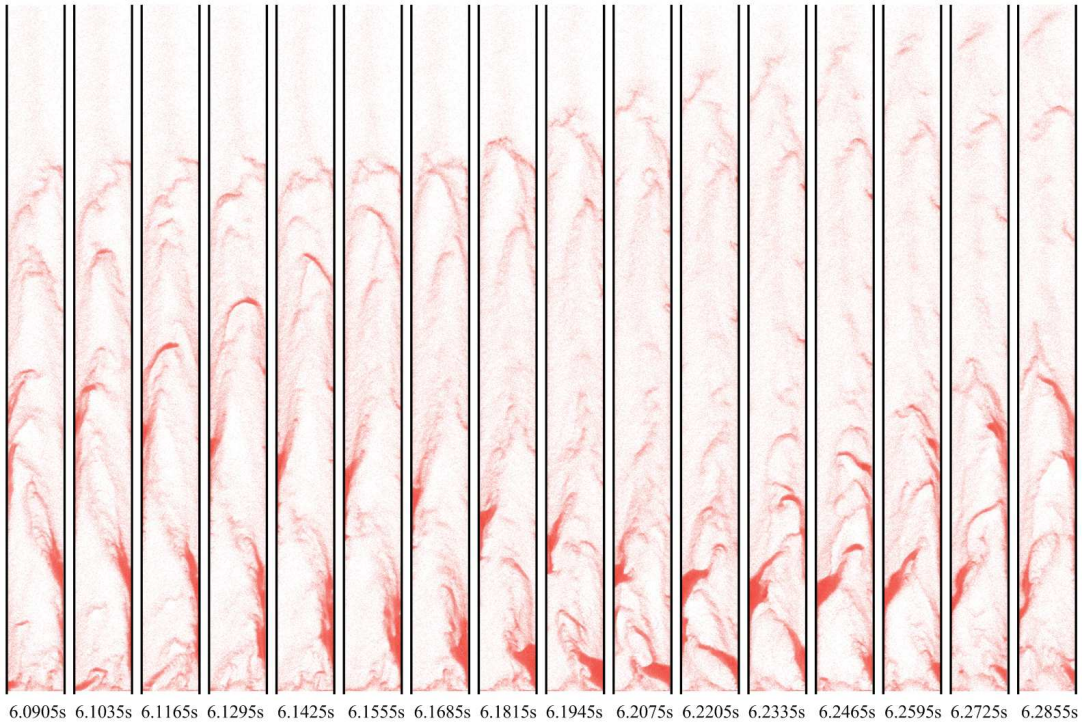


Figure 8: Evolution of flow structures in the riser of circulating fluidized beds.

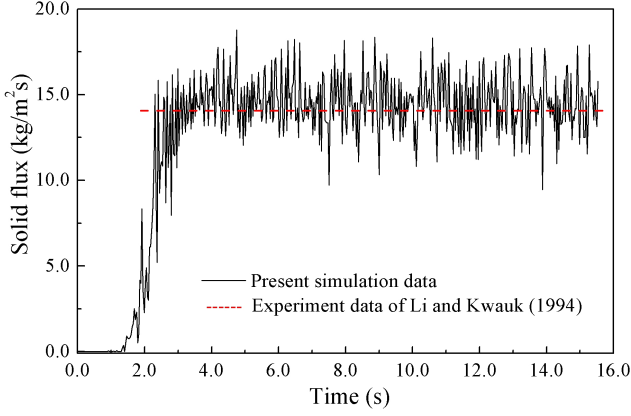


Figure 9: Evolution of the outlet solid flux in the riser of circulating fluidized beds.

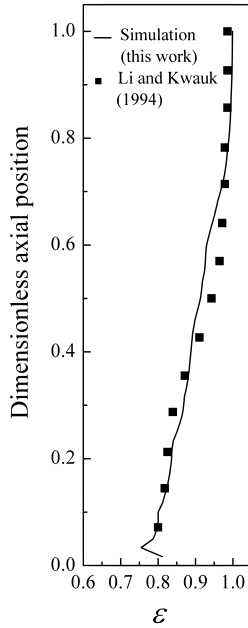


Figure 10: Axial voidage profile in the riser of circulating fluidized beds.

and Kwauk (1994). Obviously, the simulated solids fluxes ($13.8\text{kg}/(\text{m}^2\text{s})$) are in good agreement with the experimental value ($14.3\text{kg}/(\text{m}^2\text{s})$).

Figure 10 shows the comparison of the axial voidage profiles between the simulated results and the experimental data of Li and Kwauk (1994). The simulated profiles are calculated based on time-averaged from $4.0\text{s}\sim 6.6\text{s}$. The predicted sigmoid distribution of voidage in the axial direction is in reasonable agreement with experimental results, and the deviation may be partly ascribed to the unrealistic setup of inlet and outlet boundary conditions in the 2D simulation.

Figure 11 shows the comparison of the radial voidage profiles between the simulated results and the experimental correlations proposed by Tung et al. (1988). The simulated profiles are also calculated based on time-averaged from $4.0\text{s}\sim 6.6\text{s}$, which are in good agreement with empirical correlations in the core region, but overpredict the voidage in the annulus region. The coexis-

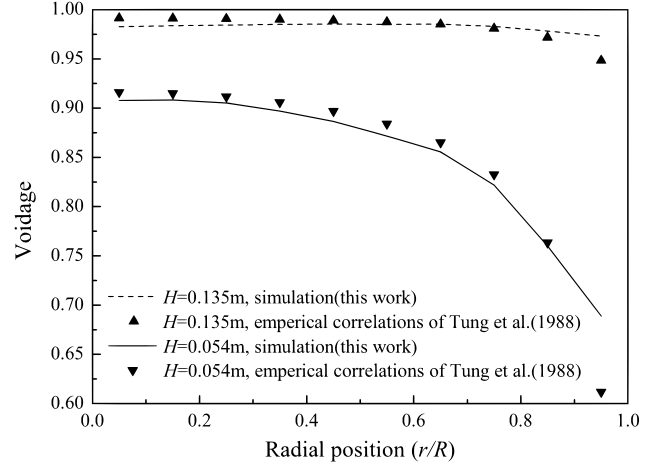


Figure 11: Radial voidage profiles in the riser of circulating fluidized beds.

tence of a dense annulus and a dilute core can be recognized, and the radial profile in the top region is larger than that in the bottom region. This implies that we have successfully captured a region with the coexistence of a dilute section at the top and a dense section at the bottom.

4. Discussion and conclusions

In this paper, a new numerical modeling method is presented for discrete particle simulation of gas-solid fluidization; while the lattice Boltzmann method is applied to model the gas flow at a scale larger than the particles, the time-driven hard-sphere model is employed to describe the motion of individual particles and the EMMS drag is used to correct gas-solid interaction. The bubble formation of a single jet into the fluidized bed and the heterogeneous flow structures in the riser of a circulating fluidized bed are simulated successfully by the proposed approach.

Although the simulated results of the proposed approach seem reasonable, the current investigation is still very preliminary. The following aspects need to be clarified further:

- *The corresponding macroscopic equations of the modified LBE.* At present, the immersed boundary method is introduced to the framework of LBM by an additional collision term to ensure that the LBE varies smoothly between the nodes occupied by pure fluid or by pure solid. This is a convenient approximation but lacks rigorous theoretical derivation. The exact form of the LBE presenting the volume-averaged N-S equation for the gas flow in DPS is not yet to be established.
- *Gas-solid coupling.* The drag force between gas-solid may be still a source of controversy in DPS due to the uncertainty and the variety of different options. Although the present work only considers no-slip discrete force ($\gamma\Omega_i^s$) with the EMMS drag correction factor (ω) as a source term (Eq. (23)), it is very flexible to incorporate other source terms or corrections into the framework of LBE. In addition to ω , which accounts for the effect of non-uniform

particle distribution, the gas velocity distribution below the lattice scale, which is fully resolved in DNS but neglected in this work, may have to be accounted for in a simplified way.

- *Fully three-dimensional simulation.* For simplicity of implementation, the current simulation lies in the restriction of two-dimensional fluid and three-dimensional individual spherical particles, and then it can be regarded as a quasi-three-dimensional simulation. Further, its extension to three-dimensions is straightforward in principle, namely using the three-dimensional lattice Boltzmann models (i.e. D3Q15, D3Q19 and D3Q27) (d’Humières et al., 2002) for gas flows. For three-dimensional physical problems of interest, despite the relatively high numerical efficiency of LBM and TDHS, excessive computational cost is still required. Naturally, we will resort to parallel computation due to the advantage of the natural parallelisms inherent in LBM and TDHS. Therefore, implementing three-dimensional massive parallel computation of the proposed model is highly desirable in future.
- *Turbulence.* Two-dimensional LES just provides a starting point for modeling high Re number gas flows and probably makes no sense here since the turbulence is inherently three-dimensional in fluidized beds.

In closing, LBM preserves the advantages of explicit methods in terms of fast speed and parallelism. While, time-driven hard-sphere model, which can be regarded as a combination of molecular dynamics (MD) and direct simulation Monte Carlo (DSMC) (Bird, 1994), inherits the virtue of computational efficiency in DSMC and physical picture in MD. Therefore, it can be expected that the proposed approach, combining LBM and TDHS, should be a fast numerical method, especially for highly parallel computing. In addition, we would like to point out that the proposed LBM based fluid flow solver can be combined with other solid phase solvers, such as DEM, DSMC (Liu and Lu, 2009), smoothed particle hydrodynamics (SPH) (Gingold and Monaghan, 1977; Monaghan, 1992; Xiong et al., 2011), and particle-in-cell (PIC) (Snider, 2001). We would like to extend the present method to complex cases involving non-spherical particles in the future work.

Notation

c	lattice speed, m/s
\mathbf{c}	unit velocity of lattice, m/s
C_{d0}	drag coefficient, kg/(m ³ s)
c_s	speed of sound, m/s
C_s	Smagorinsky constant number
d_p	solid particle diameter, m
e	coefficient of restitution
f	distribution functions
\mathbf{F}	force, m/s ²
f_i^{eq}	particle equilibrium distribution function
\mathbf{g}	gravitational acceleration, m/s ²
h	cell or lattice size, m
H	bed height, m

m	mass of solid particle, kg
n_{tot}	number of particles in a cell
N	total number of solid particles in the simulation
\mathbf{P}	position of solid particle, m
Q_{ij}	momentum fluxes
r	radius of solid particle, m
r_{inj}	orifice width, m
Re_p	particle Reynolds number
S_{ij}	strain rate tensor, s ⁻¹
t	time, s
Δt	time step, s
\mathbf{u}	gas velocity, m/s
\mathbf{v}	particle velocity, m/s
v_{inj}	injection velocity, m/s
v_{inlet}	gas velocity at the inlet, m/s
v_{mf}	minimum fluidization velocity, m/s
V_p	volume of particle, m ³
W	bed width, m
\mathbf{x}	position of lattice, m
Δx	grid size, m

Greek letters

β	drag coefficient, kg/(m ³ s)
ε	voidage
ε_g	gas volume fractions
ε_s	solid volume fractions
ε_{2d}	two dimensional porosity
ε_{3d}	three dimensional porosity
γ	weighting function
μ_g	gas viscosity, kg/(m s)
ν	kinematic viscosity, m ² /s
θ_s	initial solids volume fraction
ρ_g	gas density, kg/m ³
ρ_s	solid density, kg/m ³
ω	lattice weight or drag correction factor
Ω	collision term

Subscripts

1, 2	the numbers of solid particles
c	collion
d	drag
e	turbulent eddy or average equivalent
g	gas phase
i	the i th direction of lattice discrete velocity
k	the k th solid particle
p	particle
pre	pre-estimated
s	solid phase
t	total
x	x-direction
y	y-direction

Abbreviations

BGK	Bhatnagar-Gross-Krook
CFB	Circulating Fluidized Beds
CFBC	Circulating Fluidized Bed Combustion
CFD	Computational Fluid Dynamics
DEM	Discrete Element Method

DPS	Discrete Particle Simulation
DNS	Direct Numerical Simulation
DSMC	Direct Simulation Monte Carlo
D2Q9	2-Dimensional 9-Velocity Lattice Boltzmann Model
D3Q15	3-Dimensional 15-Velocity Lattice Boltzmann Model
D3Q19	3-Dimensional 19-Velocity Lattice Boltzmann Model
D3Q27	3-Dimensional 27-Velocity Lattice Boltzmann Model
EMMS	Energy Minimization Multi-Scale
FCC	Fluid Catalytic Cracking
LGA	Lattice Gas Automata
LBE	Lattice Boltzmann Equation
LBM	Lattice Boltzmann Method
LES	Large Eddy Simulation
MD	Molecular Dynamics
PBE	Population Balance Equation
PIC	Particle-In-Cell
QBMM	Quadrature-Based Moment Methods
SGS	Sub-Grid Scale
SPH	Smoothed Particle Hydrodynamics
TDHS	Time-Driven Hard-Sphere
TFM	Two-Fluid Model

Acknowledgement

This work is financially supported by the National Natural Science Foundation of China under Grants No. 21106155, the Specialized Fund from the Youth Innovation Promotion Association of the Chinese Academy of Science and the Chinese Academy of Sciences under Grant No. XDA07080303. We would like to thank Prof. Junwu Wang for his valuable suggestions and Dr. Qingang Xiong for useful discussions on this work.

References

- Anderson, T.B., Jackson, R., 1967. Fluid mechanical description of fluidized beds. *Industrial Engineering & Chemistry Fundamentals* 6, 527-539.
- Aidun, C.K., Clausen, J.R., 2010. Lattice-Boltzmann method for complex flows. *Annual Review of Fluid Mechanics* 42, 439-472.
- Bhatnagar, P.L., Gross, E.P., Krook, M., 1954. A model for collision processes in gases. I. Small amplitude processes in charged and neutral one-component systems. *Physical Review* 94, 511-525.
- Bird, G.A., 1994. *Molecular gas dynamics and the direct simulation of gas flows*. Oxford University Press, Oxford.
- Bokkers, G.A., Annaland, M.V.S., Kuipers, J.A.M., 2004. Mixing and segregation in a bidisperse gas-solid fluidised bed: a numerical and experimental study. *Powder Technology* 140, 176-186.
- Cai, P., Schiavetti, M., De Michele, G., Grazzini, G., Miccio, M., 1994. Quantitative estimation of bubble size in PFBC. *Powder Technology* 80, 99-109.
- Cammarata, L., Lettieri, P., Micale, G.D.M., Colman, D., 2003. 2D and 3D CFD simulations of bubbling fluidized beds using Eulerian-Eulerian Models. *International Journal of Chemical Reactor Engineering* 1, 1-14.
- Chapman, S., Cowling, T.G., 1970. *The mathematical theory of non-uniform gases*. Cambridge University Press, London.
- Chen, C., Li, F., Qi, H., 2012. Modeling of the flue gas desulfurization in a CFB riser using the Eulerian approach with heterogeneous drag coefficient. *Chemical Engineering Science* 69, 659-668.
- Chen, S., Doolen, G.D., 2003. Lattice Boltzmann method for fluid flows. *Annual Review of Fluid Mechanics* 30, 329-364.
- Chen, S., Shi, B., Liu, Z., He, Z., Guo, Z.L., Zheng, C., 2004. Lattice-Boltzmann simulation of particle-laden flow over a backward-facing step. *Chinese Physics* 13, 1657-1664.
- Chu, K., Yu, A., 2008a. Numerical simulation of complex particle-fluid flows. *Powder Technology* 179, 104-114.
- Chu, K., Yu, A., 2008b. Numerical simulation of the gas-solid flow in three-dimensional pneumatic conveying bends. *Industrial & Engineering Chemistry Research* 47, 7058-7071.
- Chu, K., Wang, B., Yu, A., Vince, A., Barnett, G.D., Barnett, P.J., 2009a. CFD-DEM study of the effect of particle density distribution on the multi-phase flow and performance of dense medium cyclone. *Minerals Engineering* 22, 893-909.
- Chu, K., Wang, B., Yu, A., Vince, A., 2009b. CFD-DEM modelling of multi-phase flow in dense medium cyclones. *Powder Technology* 193, 235-247.
- Chu, K., Wang, B., Xu, D., Chen, Y., Yu, A., 2011. CFD-DEM simulation of the gas-solid flow in a cyclone separator. *Chemical Engineering Science* 66, 834-847.
- Cook, B.K., Noble, D.R., Williams, J.R. 2004. A direct simulation method for particle-fluid systems. *Engineering Computations* 21, 151-168.
- Cundall, P., Strack, O., 1979. A discrete numerical model for granular assemblies. *Geotechnique* 29, 47-65.
- Davidson, J.F., Harrison, D., 1963. *Fluidised particles*. Cambridge University Press, London.
- Darabi, P., Pougatch, K., Salcudean, M., Grecov, D., 2011. DEM investigations of fluidized beds in the presence of liquid coating. *Powder Technology* 214, 365-374.
- Deen, N.G., Van Sint Annaland, M., Van der Holf, M.A., Kuipers, J.A.M., 2007. Review of discrete particle modeling of fluidized beds, *Chemical Engineering Science* 62, 28-44.
- Desjardins, O., Fox, R., Villedieu, P., 2008. A quadrature-based moment method for dilute fluid-particle flows. *Journal of Computational Physics* 227, 2514-2539.
- Feng, Y., Han, K., Owen, D. 2007. Coupled lattice Boltzmann method and discrete element modelling of particle transport in turbulent fluid flows: Computational issues. *International Journal for Numerical Methods in Engineering* 72, 1111-1134.
- Filippova, O., Hanel, D., 1997. Lattice-Boltzmann simulation of gas-particle flow in filters. *Computers & Fluids* 26, 697-712.
- d’Humières, D., Ginzburg, I., Krafczyk, M., Lallemand, P., Luo, L., 2002. Multiple-relaxation-time lattice Boltzmann models in three dimensions. *Philosophical transactions of the Royal Society of London A* 360, 437-451.
- Fox, R., 2008. A quadrature-based third-order moment method for dilute gas-particle flows. *Journal of Computational Physics* 227, 6313-6350.
- Fox, R.O., 2009a. Higher-order quadrature-based moment methods for kinetic equations. *Journal of Computational Physics* 228, 7771-7791.
- Fox, R.O., 2009b. Optimal moments sets for multivariate direct quadrature method of moments. *Industrial & Engineering Chemistry Research* 48, 9686-9696.
- Garg, R., Galvin, J., Li, T., Pannala, S., 2012. Open-source MFI-X-DEM software for gas-solids flows: Part I-Verification studies. *Powder Technology* 220, 122-137.
- Geng, Y., Che, D., 2011. An extended DEM-CFD model for char combustion in a bubbling fluidized bed combustor of inert sand. *Chemical Engineering Science* 66, 207-219.
- Gidaspow, D., 1994. *Multiphase flow and fluidization: continuum and kinetic theory descriptions*. Academic Press, New York.
- Gidaspow, D., Jiradilok, V., 2009. *Computational techniques: the multiphase CFD approach to fluidization and green energy technologies*, Nova Science Publishers, New York.
- Gingold, R., Monaghan, J., 1977. Smoothed particle hydrodynamics: theory and application to non-spherical stars. *Monthly Notices of the Royal Astronomical Society* 181, 375-389.
- Goniva, C., Kloss, C., Deen, N.G., Kuipers, J.A.M., Pirker, S., 2012. Influence of rolling friction on single spout fluidized bed simulation. *Particuology* 10, 582-591.
- Gopalakrishnan, P., Tafti, D., 2013. Development of parallel DEM for the open source code MFI-X. *Powder Technology* 35, 33-41.
- Gui, N., Fan, J., Luo, K., 2008. DEM-LES study of 3-D bubbling fluidized bed with immersed tubes. *Chemical Engineering Science* 63, 3654-3663.
- Guo, Z.L., Zhao, T.S., 2002. Lattice Boltzmann model for incompressible flows through porous media. *Physical Review E* 66, 036304.
- Guo, Z.L., Zheng, C.G., Shi, B.C., 2002. Discrete lattice effects on the forcing term in the lattice Boltzmann method. *Physical Review E* 65, 046308.
- Hoomans, B.P.B., Kuipers, J.A.M., Briels, W.J., Van Swaaij, W.P.M., 1996. Discrete particle simulation of bubble and slug formation in a two-dimensional gas-fluidised bed: A hard-sphere approach. *Chemical Engineering Science* 51, 4103-4114.

- ing Science 51, 99-118.
- Hopkins, M.A., Louge, M.Y., 1991. Inelastic microstructure in rapid granular flows of smooth disks. *Physics of Fluids A: Fluid Dynamics* 3, 47-57.
- Hu, H., Joseph, D. D., Crochet, M.J., 1992. Direct simulation of fluid particle motion. *Theoretical and Computational Fluid Dynamics* 3,285-306.
- Ishii, M., 1975. Thermo-fluid dynamic theory of two-phase flow. Eyrolles, Paris.
- Krafczyk, M., Tolke, J., Luo, L.S., 2003. Large-eddy simulations with a multiple-relaxation-time LBE model. *International Journal of Modern Physics B* 17, 33-40.
- Kuang, S., Chu, K., Yu, A., Zou, Z., Feng, Y., 2008. Computational investigation of horizontal slug flow in pneumatic conveying. *Industrial & Engineering Chemistry Research* 47, 470-480.
- Lan, X., Xu, C., Wang, G., Wu, L., Gao, J., 2009. CFD modeling of gas-solid flow and cracking reaction in two-stage riser FCC reactors. *Chemical Engineering Science* 64, 3847-3858.
- Li, F., Song, F., Benyahia, S., Wang, W., Li, J., 2012. MP-PIC simulation of CFB riser with EMMS-based drag model. *Chemical Engineering Science* 82, 104-113.
- Li, J., Kuipers, J., 2003. Gas-particle interactions in dense gas-fluidized beds. *Chemical Engineering Science* 58, 711-718.
- Li, J., Kwauk, M., 1994. Particle-fluid two-phase flow: the energy-minimization multi-scale method. Metallurgical Industry Press, Beijing.
- Li, T., Guenther, C., 2012. MFIX-DEM simulations of change of volumetric flow in fluidized beds due to chemical reactions. *Powder Technology* 220, 70-78.
- Li, T., Garg, R., Galvin, J., Pannala, S., 2012a. Open-source MFIX-DEM software for gas-solids flows: Part II-Validation studies. *Powder Technology* 220, 138-150.
- Li, T., Gopalakrishnan, P., Garg, R., Shahnam, M., 2012b. CFD-DEM study of effect of bed thickness for bubbling fluidized beds. *Particology* 10, 532-541.
- Liu, H., Lu, H., 2009. Numerical study on the cluster flow behavior in the riser of circulating fluidized beds. *Chemical Engineering Journal* 150, 374-384.
- Lu, B., Wang, W., Li, J., 2011. Eulerian simulation of gas-solid flows with particles of Geldart groups A,B and D using EMMS-based meso-scale model. *Chemical Engineering Science* 66, 4624-4635.
- Ma, J., Ge, W., Wang, X., Wang, J., Li, J., 2006. High-resolution simulation of gas-solid suspension using macro-scale particle methods. *Chemical Engineering Science* 61, 7096-7106.
- Mazzei, L., 2011. Limitations of quadrature-based moment methods for modeling inhomogeneous polydisperse fluidized powders. *Chemical Engineering Science* 66, 3628-3640.
- McNamara, G.R., Zanetti, G., 1988. Use of the Boltzmann equation to simulate lattice-gas automata. *Physical Review Letters* 61, 2332-2335.
- Mikami, T., Kamiya, H., Horio, M., 1998. Numerical simulation of cohesive powder behavior in a fluidized bed. *Chemical Engineering Science* 53,1927-1940.
- Monaghan, J., 1992. Smoothed Particle Hydrodynamics. *Annual Review of Astronomy and Astrophysics* 30, 543-574.
- Nieuwland, J.J., Veenendaal, M.L., Kuipers, J.A.M., Van Swaaij, W.P.M., 1996. Bubble formation at a single orifice in gas-fluidised beds. *Chemical Engineering Science* 51, 4087-4102.
- Noble, D.R., Torczynski, J.R., 1998. A lattice-Boltzmann method for partially saturated computational cells. *International Journal of Modern Physics C* 9, 1189-1201.
- Ouyang, J., Li, J., 1999a. Particle-motion-resolved discrete model for simulating gas-solid fluidization. *Chemical Engineering Science* 54, 2077-2083.
- Ouyang, J., Li, J., 1999b. Discrete simulations of heterogeneous structure and dynamic behavior in gas-solid fluidization. *Chemical Engineering Science* 54, 5427-5440.
- Qian, Y., d'Humieres, D., Lallemand, P., 1992. Lattice BGK models for Navier-Stokes equation. *Europhysics Letters* 17, 479-484.
- Rowe, P.N., Yacono, C.X.R., 1976. The bubbling behaviour of fine powders when fluidised. *Chemical Engineering Science* 31, 1179-1192.
- Schiller, L., Naumann, A., 1935. A drag coefficient correlation. *Vdi Zeitung* 77, 318-320.
- Smagorinsky, J., 1963. General circulation experiments with the primitive equations. *Monthly Weather Review* 91, 99-164.
- Snider, D., 2001. An incompressible three-dimensional multiphase particle-in-cell model for dense particle flows. *Journal of Computational Physics* 170, 523-549.
- Sterling J.D., Chen S., 1996. Stability analysis of lattice Boltzmann methods. *Journal of Computational Physics* 123, 196-206.
- Su, J., Gu, Z., Xu, X., 2011. Discrete element simulation of particle flow in arbitrarily complex geometries. *Chemical Engineering Science* 66, 6069-6088.
- Sungkorn, R., Derksen, J.J., Khinast, J.G., 2011. Modeling of turbulent gas-liquid bubbly flows using stochastic Lagrangian model and lattice-Boltzmann scheme. *Chemical Engineering Science* 66, 2745-2757.
- Tsuji, Y., Kawaguchi, T., Tanaka, T., 1993. Discrete particle simulation of two-dimensional fluidized-bed. *Powder Technology* 77, 79-87.
- Tung, Y., Li, J., Kwauk, M., 1988. Radial voidage profiles in a fast fluidized bed, in: Kwauk, M., Kunii, D. (Eds.), *Fluidization '88: Science and Technology*. Science Press, Beijing, pp. 139-145.
- Wang, J., Ge, W., Li, J., 2008. Eulerian simulation of heterogeneous gas-solid flows in CFB risers: EMMS-based sub-grid scale model with a revised cluster description. *Chemical Engineering Science* 63, 1553-1571.
- Wang, L., Ge, W., Li, J., 2006. A new wall boundary condition in particle methods. *Computer Physics Communications* 174, 386-390.
- Wang, L., Zhou, G., Wang, X., Xiong, Q., Ge, W., 2010. Direct numerical simulation of particle-fluid systems by combining time-driven hard-sphere model and lattice Boltzmann method. *Particology* 8, 379-382.
- Wang, S., Lu, H., Li, X., Wang, J., Zhao, Y., Ding, Y., 2009. Discrete particle simulations for flow of binary particle mixture in a bubbling fluidized bed with a transport energy weighted averaging scheme. *Chemical Engineering Science* 64, 1707-1718.
- Wang, S., Li, X., Lu, H., Liu, G., Wang, J., Xu, P., 2011. Simulation of cohesive particle motion in a sound-assisted fluidized bed. *Powder Technology* 207, 65-77.
- Wei, M., Wang, L., Li, J., 2013. Unified stability condition for particulate and aggregative fluidization. *Exploring energy dissipation with direct numerical simulation*. *Particology* 11, 232-241.
- Wu, C., Berrouk, A.S., Nandakumar, K., 2009. Three-dimensional discrete particle model for gas-solid fluidized beds on unstructured mesh. *Chemical Engineering Journal* 152, 514-529.
- Wu, C., Cheng, Y., Ding, Y., Jin, Y., 2010. CFD-DEM simulation of gas-solid reacting flows in fluid catalytic cracking (FCC) process. *Chemical Engineering Science* 65, 542-549.
- Xie, N., Battaglia, F., Pannala, S., 2008. Effects of using two- versus three-dimensional computational modeling of fluidized beds: part I, hydrodynamics. *Powder Technology* 182, 1-13.
- Xiong, Q., Deng, L., Wang, W., Ge, W., 2011. SPH method for two-fluid modeling of particle-fluid fluidization. *Chemical Engineering Science* 66, 1859-1865.
- Xiong, Q., Li, B., Zhou, G., Fang, X., Xu, J., Wang, J., He, X., Wang, X., Wang, L., Ge, W., Li, J., 2012. Large-scale DNS of gas-solid flows on Mole-8.5. *Chemical Engineering Science* 71, 422-430.
- Xu, B., Yu, A., 1997. Numerical simulation of the gas-solid flow in a fluidized bed by combining discrete particle method with computational fluid dynamics. *Chemical Engineering Science* 52, 2785-2809.
- Xu, M., Ge, W., Li, J., 2007. A discrete particle model for particle-fluid flow with considerations of sub-grid structures. *Chemical Engineering Science* 62, 2302-2308.
- Yang, N., Wang, W., Ge, W., Li, J., 2003. CFD simulation of concurrent-up gas-solid flow in circulating fluidized beds with structure-dependent drag coefficient. *Chemical Engineering Journal* 96, 71-80.
- Yu, H., Girimaji, S.S., Luo, L., 2005. DNS and LES of decaying isotropic turbulence with and without frame rotation using lattice Boltzmann method. *Journal of Computational Physics* 209, 599-616.
- Zhao, X., Li, S., Liu, G., Yao, Q., Marshall, J.S., 2008. DEM simulation of the particle dynamics in two-dimensional spouted beds. *Powder Technology* 184, 205-213.
- Zhao, Y., Jiang, M., Liu, Y., Zheng, J., 2009. Particle-scale simulation of the flow and heat transfer behaviors in fluidized bed with immersed tube. *AIChE Journal* 55, 3109-3124.
- Zhao, Y., Ding, Y., Wu, C., Cheng, Y., 2010. Numerical simulation of hydrodynamics in downers using a CFD-DEM coupled approach. *Powder Technology* 199, 2-12.
- Zhou, H., Flamant, G., Gauthier, D., 2004a. DEM-LES of coal combustion in a bubbling fluidized bed. Part I: gas-particle turbulent flow structure. *Chemical Engineering Science* 59, 4193-4203.

- Zhou, H., Flamant, G., Gauthier, D., 2004b. DEM-LES simulation of coal combustion in a bubbling fluidized bed Part II: coal combustion at the particle level. *Chemical Engineering Science* 59, 4205-4215.
- Zhu, H., Zhou, Z., Yang, R., Yu, A., 2007. Discrete particle simulation of particulate systems: theoretical developments, *Chemical Engineering Science* 62, 3378-3396.
- Zhu, H., Zhou, Z., Yang, R., Yu, A., 2008. Discrete particle simulation of particulate systems: A review of major applications and findings. *Chemical Engineering Science* 63, 5728-5770.